Improved Puncture Resistance in Textile Assemblages Achieved with Shear Thickening Fluid (STF) Intercalation and Inter-layer Friction Enhancement

Journal:	*ACS Applied Materials & Interfaces*
Manuscript ID	Draft
Manuscript Type:	Article
Date Submitted by the Author:	n/a
Complete List of Authors:	Cwalina, Colin; University of Delaware, Chemical Engineering Dombrowski, Richard; University of Delaware, Chemical Engineering Wagner, Norman J.; University of Delaware, Chemical Engineering

Improved Puncture Resistance in Textile Assemblages Achieved with Shear Thickening Fluid (STF) Intercalation and Inter-layer Friction Enhancement

Colin D. Cwalina, Richard D. Dombrowski, and Norman J. Wagner

Department of Chemical and Biomolecular Engineering, University of Delaware, Newark, DE 19716, USA

Submitted to: ACS Applied Materials & Interfaces

Abstract

Protective textiles designed for ballistic applications are susceptible to defeat from puncture threats. Intercalation of fabrics with shear thickening fluids (STF) can improve the ballistic and stab protection of these soft armor materials without compromising weight or flexibility. The mechanism for this improved performance is due to viscous dissipation within the fluid and a decrease in yarn mobility within individual fabric layers preventing windowing of the penetrator. However, the role of inter-layer friction, e.g. friction between textile layers, on the ability of the assemblage as a whole to dissipate energy is not well understood. This work elucidates the effect of STF intercalation and inter-layer friction enhancement on the resistance of ballistic and correctional aramid fabrics to hypodermic needle puncture under quasi-static loading. By itself, STF intercalation of Kevlar® fabrics was observed to improve energy dissipation regardless of the fabric architecture or needle gauge. Enhancing inter-layer friction resulted in a more complex behavior where energy dissipation was found to depend on the fabric architecture and the needle size. The results of this work demonstrate the potential to improve

the puncture resistance of a ballistic textile through control of both intra-layer and inter-layer friction, which is valuable for the advancement of multi-threat protective materials.

Introduction

High strength-to-weight woven aramid fabrics have found prevalent application in soft armor and personal protective equipment. It has been demonstrated that the material properties of the fibers and the geometry of the fabric weave combine to produce the observed ballistic response [1, 2]. For ballistic impacts, yarn pull-out has been shown to be the dominant energy dissipation mechanism [3, 4]. However, in situations where the projectile is of higher gauge, ballistic fabrics are susceptible to "wedge through", or "windowing", whereby the projectile can push aside and slip by yarns rather than pulling them through the weave and/or breaking them [5-7]. A reduction in the mobility of yarns has been shown to improve energy absorption by forcing a projectile to engage and break more yarns [8]. With lower gauge ballistic projectiles, earlier studies showed that high inter-yarn friction leads to earlier yarn breakage and a reduction in ballistic energy dissipation [9]. These studies point to the importance of controlling inter-yarn friction and suggest the maximum ballistic resistance will be achieved by optimizing inter-yarn friction.

Several efforts have been made to improve the penetration resistance of ballistic fabrics through intercalation of the fabric with shear thickening fluid (STF), which leads to a unique, rate dependent inter-yarn friction. Shear thickening colloidal dispersions exhibit a reversible increase in viscosity with increasing shear rate or shear stress [10-15]. Upon relaxation of the applied stress, the suspension microstructure is restored on the rapid time scale of Brownian

motion and the material returns to a fluid-like state [10]. STFs have been successfully intercalated into Kevlar® to improve ballistic and stab performance as STF-Armor™ [15-18]. This effect has been studied and reproduced by numerous other groups [19-22]. STFs are distinguished from dilatant suspensions, which dissipate energy through frictional interactions as they must expand their total volume in order to flow [23]. Composites of dilatant materials with ballistic fabrics have also been proposed for improving ballistic resistance [24], but have not shown improvements in puncture resistance.

Lee *et al.* [18] performed ballistic experiments on a woven Kevlar® fabric intercalated with a colloidal STF of silica nanoparticles dispersed in polyethylene glycol. STF-treated targets showed comparable penetration resistance and flexibility to neat targets while requiring fewer layers and reduced mass as the STF constrained yarns being pulled through the fabric. Kalman *et al.* [15] studied the effect of particle hardness on the penetration resistance of fabrics intercalated with dry particles and STF. The results demonstrated that viscous stress transfer, friction, and particle abrasion of the filaments are all relevant mechanisms in the energy dissipation process. Decker *et al.* [14] showed that the hard STF particles indent and create grooves in the Kevlar® filaments when deformed. McAllister *et al.* [25] measured the energy dissipated by nanoindentation of the Kevlar® under various deformation modes. Indeed, the shear thickening effect itself is found to increase energy absorption [26]. Decker *et al.* [14] investigated the stab resistance of neat and STF-treated Kevlar® using the NIJ spike. At equal areal densities, STF-treated Kevlar® offered superior stab resistance over its neat counterpart. The reduction in yarn mobility by the incorporation of STF was shown to successfully resist windowing by the spike. This body of prior work shows that a nanocomposite-fabric system that

controls the rate-dependent inter-yarn friction can be engineered to improve both ballistic and stab protection.

Frictional energy dissipation upon a ballistic impact or puncture event in an aramid fabric can take many forms, including intra-yarn, inter-yarn, inter-layer, and projectile-fabric. The effects of friction have been well documented for a single layer of fabric, particularly for ballistic impacts. Cheeseman and Bogetti [5] reviewed several factors that influence the penetration resistance of ballistic fabrics. Both yarn-yarn and yarn-projectile friction were found to play a role in the energy dissipation process during impact. Further, material properties such as the elastic modulus and tensile strength of the yarn itself have a significant influence on the overall effect of friction between yarns, and are critical for maintaining fabric integrity throughout the impact event [27].

Impact modeling efforts have also produced insights into the role of friction within a ballistic fabric. Friction has been shown to enhance the energy dissipation during a ballistic impact through three mechanisms: transfer of the projectile's energy into kinetic energy of yarns, transfer of the projectile's energy into strain energy within yarns, and frictional sliding of yarns at contact points [28, 29]. Concerning the latter, very high inter-yarn friction was shown to lead to premature breakage of yarns, while low inter-yarn friction enables windowing. Thus, an optimum coefficient of inter-yarn friction was identified for the particular fabric under study [30]. A recent, detailed numerical simulation of the ballistic resistance of a single layer of Kevlar® KM2 provides a quantitative understanding of the influence of intra-layer friction on reducing windowing during ballistic impact [31].

Modifying the surface treatment of fabrics to alter the level of interfacial friction has been studied experimentally. A review of these efforts is warranted for the context of the present work. Briscoe and Motamedi [32] studied the effects of surface friction characteristics of aramid fabrics on their ballistic performance. Surface treatments were shown to affect the overall modulus of the fabric, which changes the wave velocity and stress propagation away from the impact site. Lubrication allowed for easier filament migration and a less stiff response. Fabrics with enhanced surface friction were found to have improved ballistic performance compared with those that were lubricated. Other interfacial modifications have included thermoplastic impregnation [33], thermally sprayed ceramic coatings [34], fluorinated polymer finishes [35], and natural rubber latex coatings [36]. The purpose of such surface alterations was to restrict the motion of yarns within the fabric during an impact.

Of significant technological interest is the resistance of protective fabrics to threats such as hypodermic needles. Termonia [37] numerically modeled the resistance of fibrous structures to needle puncture. The analysis concluded that needle puncture occurs through four distinct stages: (i) deflection of the fabric due to contact pressure from the needle; (ii) puncture of the fabric as the needle tip slips into an inter-fiber spacing; (iii) friction of the fabric against the translating needle shaft; and (iv) slippage of the needle shaft through the fabric once the barrel of the needle breaches the fabric.

Although much is known concerning the role of friction during a ballistic impact into protective fabrics, particularly within a single layer (for a discussion see Kalman *et al.* [15]), there are relatively few experimental studies of fabric puncture involving hypodermic needles. The work of Houghton *et al.* [38] confirmed many of the qualitative theoretical predictions of

fabric behavior under needle puncture. Dombrowski and Wagner [39] further showed the direct effect of needle gauge on the observed amount of energy dissipated.

Another potentially important parameter concerning puncture resistance of fabric assemblies is the role of *inter-layer* friction, i.e., between adjacent layers within assemblages of textiles. As protective devices are generally comprised of multiple layers, understanding how the inter-layer friction affects the energy dissipation of the entire assemblage is important for their design and optimization. The present work investigates the effects of restricting intra-layer and inter-layer fiber mobility on the quasi-static puncture resistance of fabric assemblages comprised of ballistic and correctional woven aramid fabrics over a range of needle gauges. Intra-layer fiber mobility is restricted by intercalating the fabric with STF and the relative motion of fibers in adjacent fabric layers is restricted by increasing the coefficient of friction between layers using polyurethane film. We first consider the effects of STF intercalation and inter-layer friction enhancement separately to gain a mechanistic understanding of their respective roles during needle puncture of a fabric assemblage. In particular, we investigate the effect of enhanced inter-layer friction on the ability of the fabric assemblages to dissipate energy as a function of the fabric architecture and the gauge of the needle. We conclude by simultaneously intercalating the textile assemblages with STF and enhancing the inter-layer friction to explore possible synergistic effects that affect the puncture resistance.

Experimental Section

Materials

The protective fabrics evaluated in this study were obtained from Barrday (Cambridge, Ontario, Canada) and were selected on the basis of having distinctly different material properties

such as denier and yarns per inch (ypi). The fabrics were woven ballistic Kevlar® Style 1025 (KM2 600 denier, 34.5 x 35 ypi) and correctional Kevlar® Style 1148 (K159 300 denier, 59 x 59 ypi) along with a commercial STF-treated Style 1148. A laboratory scale process [15] for manufacturing STF-nanocomposites was used to produce a STF-treated (Seahostar KE-P50 silica, Nippon Shokubai Co., Tokyo, Japan, in polyethylene glycol MW=200) Style 1025. Table 1 provides the relevant properties of the materials tested. BD (Becton, Dickinson, and Company) PrecisionGlide™ (Franklin Lakes, NJ) hypodermic needles of gauge 18 (1.270 mm barrel diameter) and 23 (0.641 mm) were used as well as 14 gauge (2.108 mm) Monoject™ hypodermic needles from Tyco Healthcare Group (Mansfield, MA). Note that these hypodermic needles have a cutting edge that can facilitate penetration relative to a conical cross-section typical of a spike.

Table 1. Material properties of fabrics used in this study.

Material	Designation	Denier	YPI	Areal Density (g/m^2)
Kevlar® 1025 Untreated Fabric	1025	600	34.5x35	196
Kevlar® 1025 STF-Treated Fabric	1025-STF	600	34.5x35	237
Kevlar® 1148 Untreated Fabric	1148	300	59x59	160
Kevlar® 1148 STF-Treated Fabric	1148-STF	300	59x59	171

Two different levels of inter-layer friction were studied as follows. Assemblages consisting of four layers of fabric without any interlayer material were considered *neat* assemblages. Inter-layer friction was enhanced by inserting polyurethane (PU) film from American Polyfilm (Brandford, CT) between each Kevlar® fabric layer as interlayers.

Coefficients of friction for all materials were measured against an A316 stainless steel reference using a commercial tribo-rheometry fixture similar to that described by Kavehpour and McKinley [40]. The A316 stainless steel ring was mounted to a Discovery Hybrid Rheometer (TA Instruments, New Castle, DE) and rotated at a constant angular velocity and normal force against the material of interest below. From the measured torque, the coefficient of friction was determined from Equation 1:

$$\mu = \frac{T(R_o + R_i)}{F_N(R_o^2 + R_i^2)} \quad (1)$$

where μ is the coefficient of friction, T is the measured torque, F_N is the applied normal force, and R_o and R_i are the outer and inner radii of the stainless steel ring, respectively. The measured coefficients of friction against the A316 stainless steel reference are displayed below in Table 2. The purpose of these measurements was to demonstrate that the PU provides a meaningful enhancement in the level of friction between layers when inserted into the inter-layer space.

Table 2. Coefficient of friction measured against an A316 stainless steel reference.

Material	Coefficient of Friction
1025	0.30 ± 0.03
1025-STF	0.28 ± 0.05
1148	0.12 ± 0.01
1148-STF	0.16 ± 0.01
PU	0.70 ± 0.06

Puncture Testing

The experimental apparatus used for puncture testing was a modification of the ASTM F-1342 standard. A hypodermic needle of varying gauge was used instead of the F-1342 standard

probe. Hypodermic needles are complex threats. In additional to a conical tip, they possess a continuous cutting edge that can facilitate penetration. The apparatus is shown schematically in Figure 1.

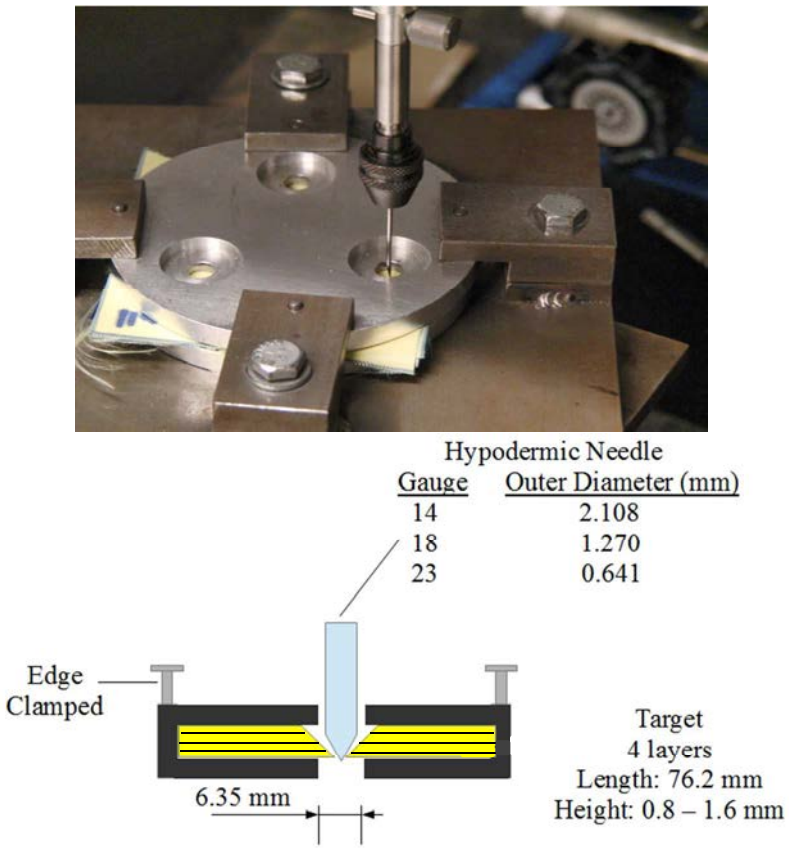

Figure 1. Experimental testing apparatus and schematic showing relevant dimensions.

The assemblages consisted of four layers of fabric and twelve replicates were obtained for each configuration. The hypodermic needle was held within a chuck and mounted to a 500 N load cell on an Instron 5965. Assemblages were loaded at a rate of 254 mm/min. The force on the needle was recorded as a function of its displacement through the lay-up. A new needle was used for every penetration experiment to insure a consistent sharpness.

Inter-layer friction was varied by the insertion of PU film between textile layers. The addition of PU film interlayers naturally adds material and mass to the assemblage. To ensure that any added energy dissipation observed was not simply a consequence of this additional material, energy dissipation was measured at PU film thicknesses of 0.0254 mm (1 mil), 0.127 mm (5 mil), and 0.254 mm (10 mil). The energy dissipation observed at these three thicknesses was then extrapolated back to zero PU thickness. This extrapolation yields the energy dissipation for a massless, infinitesimally thin interlayer of PU, i.e., for an increase of the inter-layer coefficient of friction without an increase in assemblage mass or thickness.

Results and Discussion

A typical set of loading curves is shown below in Figure 2. The lay-up in this particular set of replicates was Kevlar® 1025 penetrated by an 18 gauge (1.270 mm barrel diameter) hypodermic needle with no PU interlayer. Twelve replicates are displayed with the average force at a given value of displacement shown in bold. The modelling of Termonia [37] provides mechanistic insight into the nature of force vs. displacement measurements in a single fabric layer, although it should be noted the needles in that particular study did not possess a continuous cutting surface. The initial uptick in the force at low displacements corresponds to the deflection of yarns by the needle. This is followed by a second distinguishable region of the curve where the slope of the force vs. displacement curve is significantly larger, reflecting tensioning of the yarns. The peak in the loading curve occurs when the needle slips into an inter-fiber space, at which point the fabric has been punctured. For multi-layer fabric assemblages, puncture is found to occur sequentially rather than simultaneously. From the data in Figure 2, the initial deflection and tensioning of the yarns is fairly consistent between replicates. However, the value of the peak force and displacement at which it occurs is statistical in nature.

This phenomenon is common for fabrics which present a heterogeneous surface to the hypodermic needle penetrators [39].

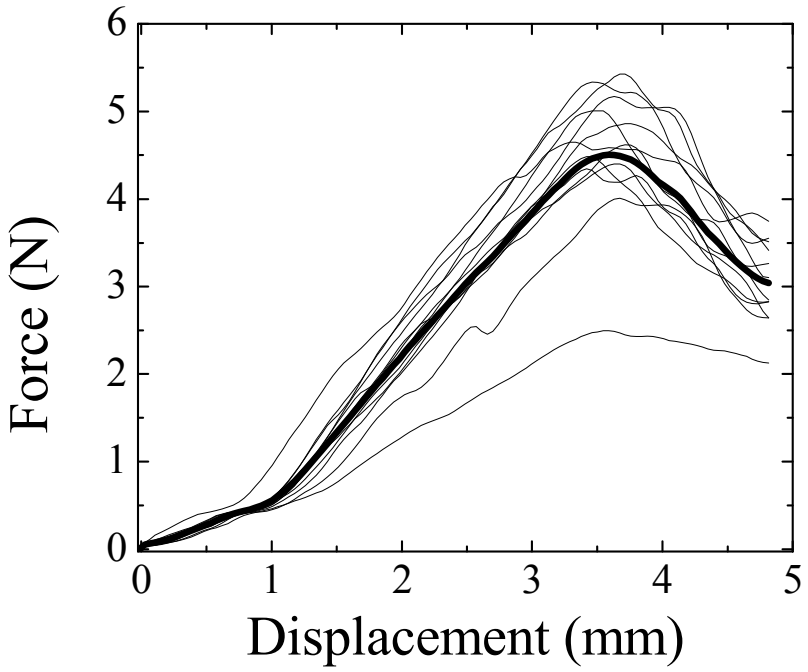

Figure 2. Twelve replicates of Kevlar® 1025 penetrated by a 1.270 mm barrel diameter (18 gauge) hypodermic needle. The average force at a given displacement is shown in bold.

We first consider the effect of STF intercalation. The loading curves for all combinations of fabric weave and needle gauge are qualitatively similar, and as such, we only show the set of curves for 1025 and 1025-STF assemblages penetrated by an 18 gauge needle in Figure 3. The peak puncture force, the displacement at which that force occurs, and the energy dissipated up to

that point are useful metrics for quantifying resistance to a puncturing threat. All three values are reported in Table 3 for each fabric and needle gauge.

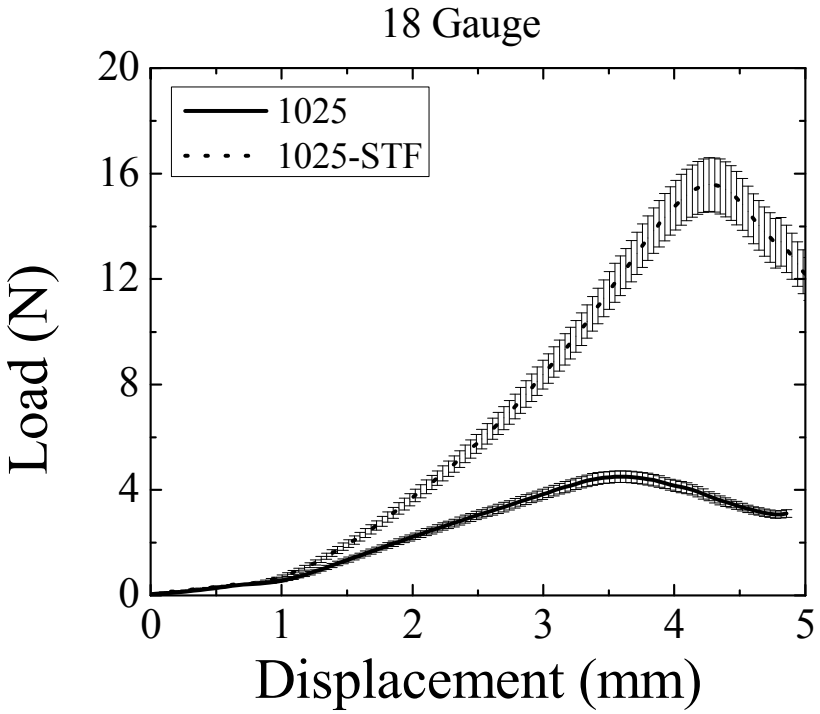

Figure 3. Loading curves for 1025 and 1025-STF assemblages penetrated by an 18 gauge needle. The solid line (untreated fabrics) and dotted line (STF-treated fabrics) are the average force at a given value of displacement recorded during the twelve replicate experiments. Error bars mark the standard error about the mean at a given value of displacement.

Table 3. Peak puncture force and energy dissipated up to that displacement for untreated and STF intercalated fabrics for various needle gauge penetrators. The numbers in parenthesis in the force and energy dissipated columns are the percentage increases for the STF intercalated assemblages over their respective untreated counterparts at a given needle gauge.

Fabric	Needle Gauge	Displacement (mm)	Force (N)	Energy Dissipated (mJ)
1025	14	4.7	17.8 ± 1.0	37.6 ± 2.1
1025-STF	14	5.0	48.6 ± 4.0 (170%)	89.9 ± 7.4 (140%)
1025	18	3.6	4.5 ± 0.2	7.3 ± 0.3
1025-STF	18	4.3	15.6 ± 1.0 (250%)	24.2 ± 1.6 (230%)
1148	18	4.0	22.1 ± 1.0	34.3 ± 1.6
1148-STF	18	4.0	35.3 ± 1.7 (60%)	52.0 ± 2.5 (50%)
1148	23	2.6	6.6 ± 0.3	7.3 ± 0.3
1148-STF	23	2.9	11.5 ± 0.5 (70%)	13.9 ± 0.6 (90%)

In all cases, STF intercalation improved the peak force as well as the energy dissipation of the lay-up. The results are consistent with previous work showing an improvement in puncture resistance with STF intercalation [38]. This increase in penetration resistance is most significant for the ballistic Style 1025 fabric. The nature of ballistic fabric weaves renders them susceptible to defeat from narrow penetrators that can window between yarns and fibers. The role of the STF-treatment in mitigating and suppressing this windowing mechanism can be understood using arguments advanced by Decker *et al.* [26] and Houghton *et al.* [38]. Upon an impact that exceeds the critical stress for shear thickening, the STF transitions to its high viscosity state. This transition to the shear-thickened state improves the energy dissipation of the

fabric, both through viscous dissipation within the STF and the restriction of yarn motion and pull-out from the fabric due to the solidification of the STF. The results here confirm prior reports that STF intercalation of ballistic fabrics can lead to significant performance enhancements in multilayer lay-ups against narrow puncture and cutting threats.

The effect of restricting the relative motion of fibers between adjacent layers is explored next through the insertion of PU film at various thicknesses between fabric layers. To separate the effect of restricting the intra-layer mobility of fibers and inter-layer mobility, only assemblages of untreated fabric are considered. A sample set of loading curves are shown in Figure 4 for 1025 assemblages with varying PU interlayer thickness penetrated by an 18 gauge needle. The peak force and energy dissipated up to that displacement are reported in Figures 5 as a function of the PU thickness for each combination of fabric weave and needle gauge. A line of best fit is shown in each graph which is extrapolated back to zero PU thickness. These are the peak force and energy dissipation values for a massless, infinitesimally thin interlayer of PU, i.e., for an increase of the inter-layer coefficient of friction without an increase in lay-up mass or thickness. The peak force and energy dissipation values for the neat assemblages and the enhanced inter-layer friction lay-ups are shown in Table 4 for comparison.

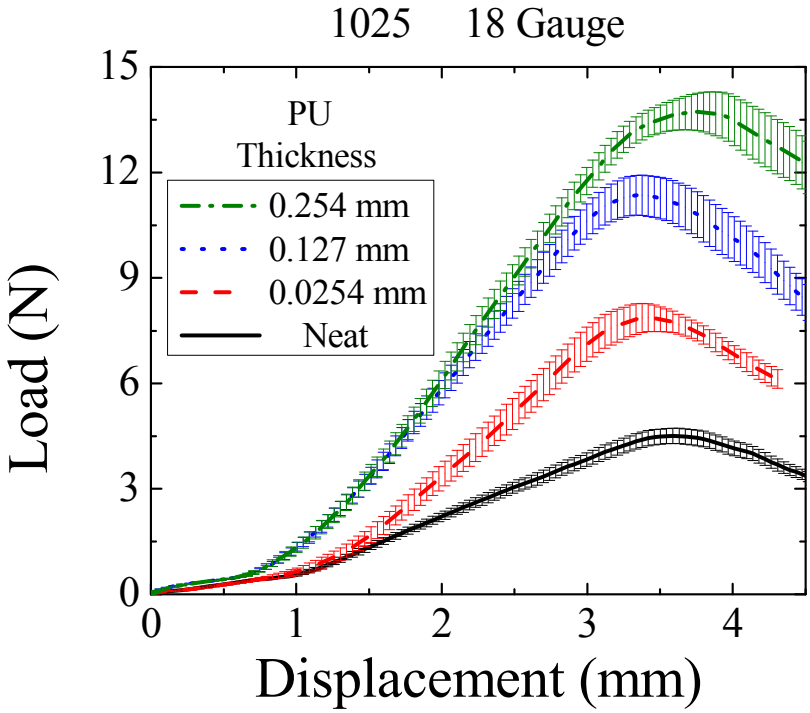

Figure 4. Loading curves for 1025 fabric assemblages with PU interlayers of varying thickness penetrated by an 18 gauge needle. The lines are the average force recorded at a given value of displacement during twelve replicate experiments. Error bars mark the standard error about the mean at a given value of displacement.

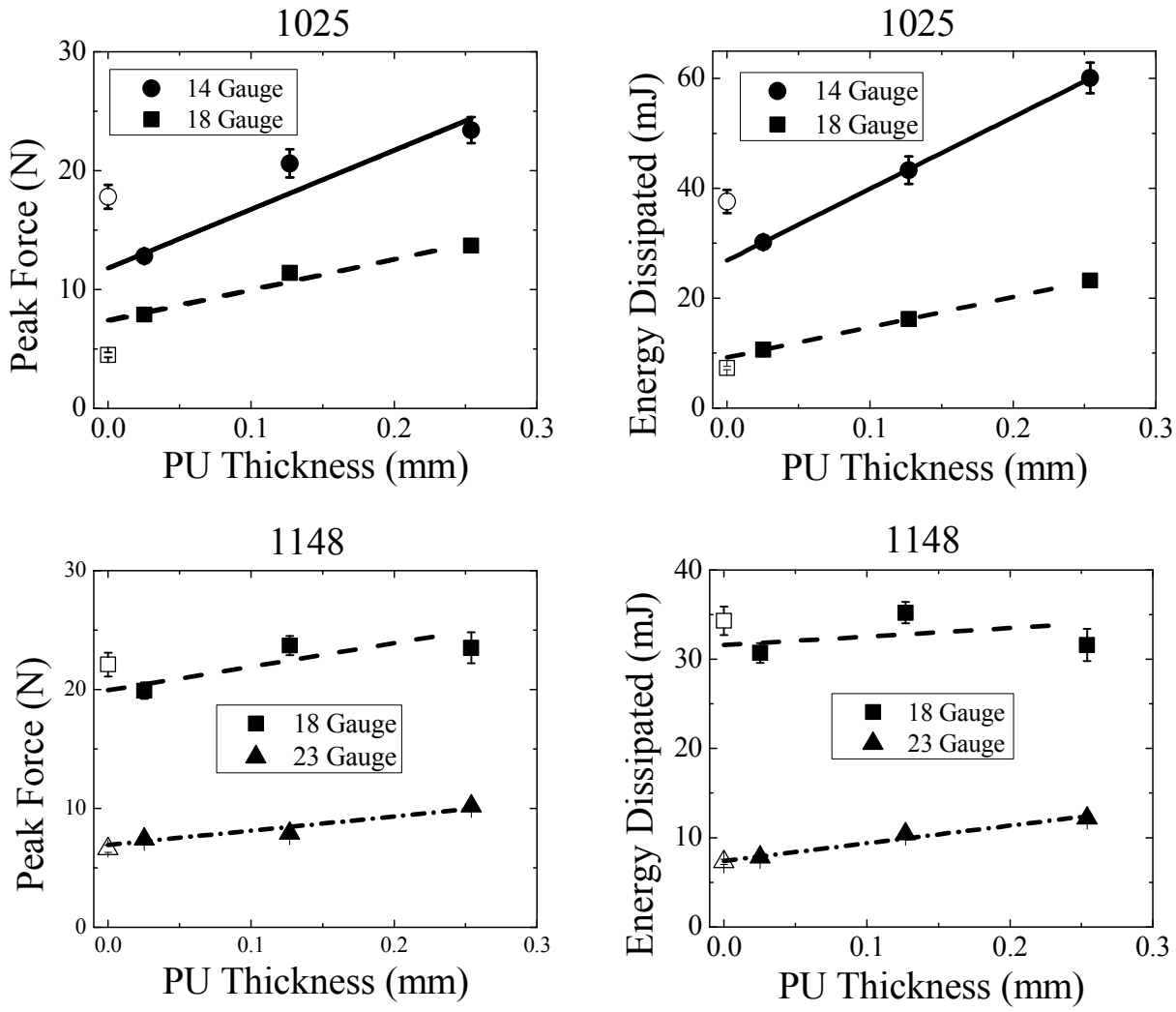

Figure 5. Peak puncture force and energy dissipated as a function of PU interlayer thickness for untreated fabrics with hypodermic needles of varying gauge (solid symbols). The lines of best fit are extrapolated back to zero PU thickness. For comparison, the peak puncture force and energy dissipation measured for the neat fabric assemblages (no PU interlayer) are shown for comparison (open symbols).

Table 4. Peak puncture force and energy dissipation measured for neat assemblages (no PU interlayers) of untreated fabric and the respective values calculated by extrapolating back to zero PU thickness. The latter values would be those expected for assemblages with an enhanced coefficient of friction between adjacent layers in the fabric assemblage.

		Neat Assemblages		Zero PU Thickness	
Fabric	**Needle Size**	**Peak Force (N)**	**Energy Dissipated (mJ)**	**Peak Force (N)**	**Energy Dissipated (mJ)**
1025	14	17.8 ± 1.0	37.6 ± 2.1	11.8 ± 1.3	26.9 ± 0.1
1025	18	4.5 ± 0.2	7.3 ± 0.3	7.6 ± 0.8	9.2 ± 0.1
1148	18	22.1 ± 1.0	34.3 ± 1.6	20.0 ± 1.6	32.1 ± 3.1
1148	23	10.2 ± 0.4	12.2 ± 0.5	6.8 ± 0.5	7.6 ± 0.4

The enhancement of inter-layer friction does not result in a universal increase in the peak puncture force or the energy dissipated. In fact, there is no statistically significant change in either peak puncture force or energy dissipation for the 1148 assemblages. For these correctional fabric assemblages, surface yarn mobility is already significantly constrained by the nature of the tight fabric weave. As such, enhancing the relative amount of friction between layers does not significantly alter the peak force or energy dissipation as there is little lateral yarn displacement during needle penetration. Without yarn displacement, there is no contribution to the peak force or energy dissipation from frictional sliding against the interlayer.

The effect of enhanced inter-layer friction is more complex with the loosely woven ballistic fabric. For the 1025 assemblages, increasing the amount of friction between layers increases the peak force and energy dissipation of the assemblages for the thinner 18 gauge needle, but enhanced inter-layer friction is detrimental for a wider 14 gauge threat. With the

ballistic weave, yarns move laterally within the plane of the fabric during the penetration event as the needle attempts to window. This lateral motion of yarns is resisted by the friction between fabric layers. A possible explanation for the complex energy dissipation behavior may be related to the rate at which yarns displace laterally against an interlayer with a higher coefficient of friction. The rate of lateral yarn displacement away from the penetrating needle is larger for the 14 gauge needle due to its wider barrel. For high levels of inter-layer friction, this may result in less yarn displacement before breakage and a reduction in the amount of the needle's energy that can be dissipated. In contrast, for the 18 gauge needle, the enhanced inter-layer friction requires the needle to exert a larger force and expend more energy to displace yarns laterally. However, the rate of lateral yarn displacement is sufficiently small so as to avoid yarn breakage. Thus, the adverse effects of increased inter-layer friction for larger barrel needles are qualitatively similar to observations of excessive inter-yarn friction promoting yarn breakage during penetration events [9, 30]. These former studies and the results of the present work suggest the penetration behavior of fabrics can be tailored by adjusting the relative amount of friction between yarns and between layers in fabric assemblages.

We conclude the discussion by examining the combined effects of STF intercalation and inter-layer friction enhancement. The peak force and energy dissipation measurements as a function of PU interlayer thickness for STF intercalated assemblages are shown in Figure 6. The extrapolated zero thickness PU peak force and energy dissipated values are compared to the neat 1025-STF and 1148-STF assemblages in Table 5.

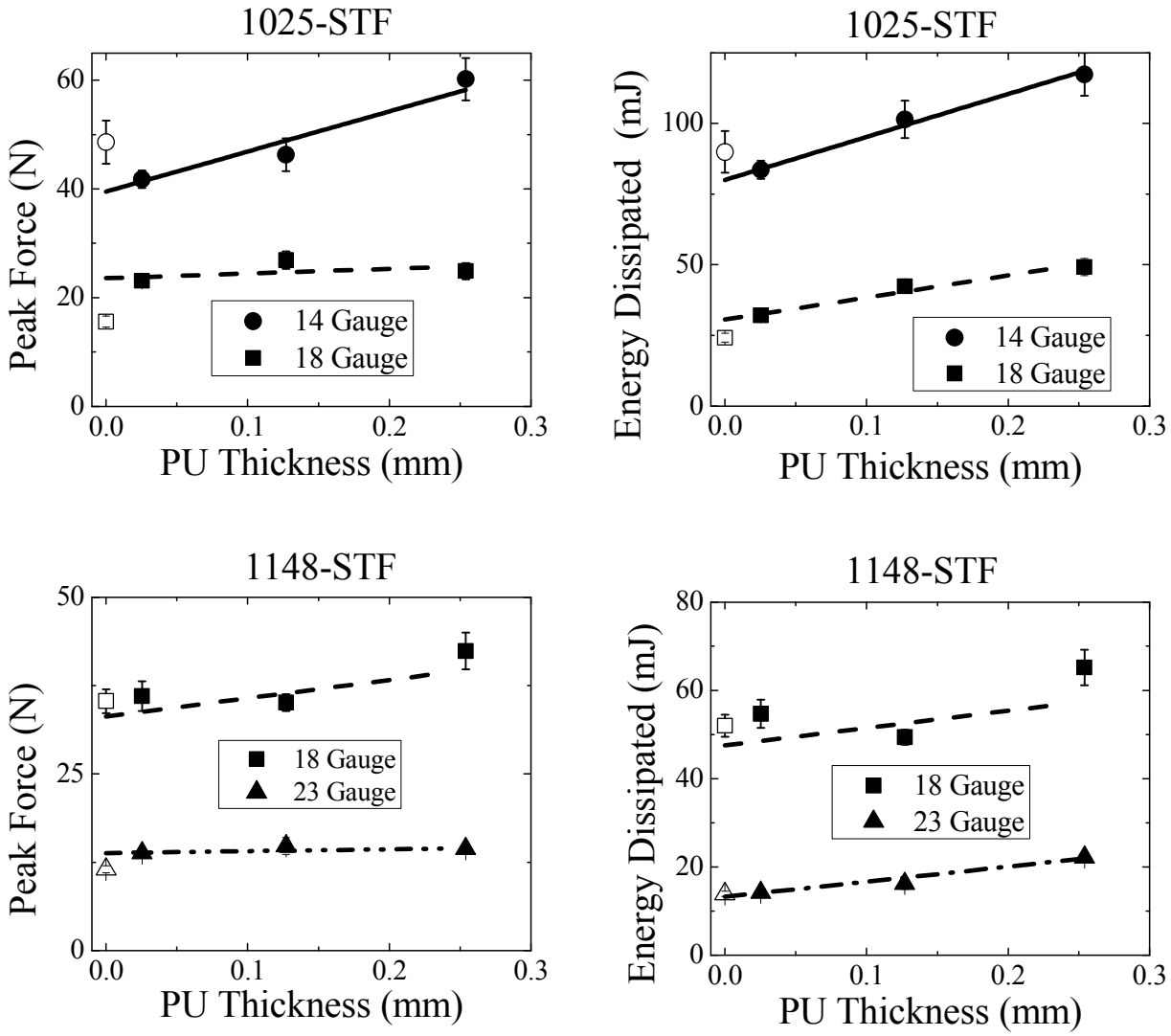

Figure 6. Peak puncture force and energy dissipated as a function of PU interlayer thickness for STF intercalated fabrics with hypodermic needles of varying gauge (solid symbols). The lines are linear extrapolations back to zero PU thickness. For comparison, the peak puncture force and energy dissipation measured for the neat fabric assemblages (no PU interlayer) are shown for comparison (open symbols).

Table 5. Peak puncture force and energy dissipation measured for neat assemblages (no PU interlayers) of fabric intercalated with STF and the respective values calculated by regressing to zero PU thickness. The latter values would be those expected for assemblages with an enhanced coefficient of friction between adjacent layers in the fabric assemblage.

		Neat Assemblages		Zero PU Thickness	
Fabric	**Needle Size**	**Peak Force (N)**	**Energy Dissipated (mJ)**	**Peak Force (N)**	**Energy Dissipated (mJ)**
1025-STF	14	48.6 ± 4.0	89.9 ± 7.4	38.3 ± 1.9	80.8 ± 1.3
1025-STF	18	15.6 ± 1.0	24.2 ± 1.6	24.0 ± 2.1	31.2 ± 1.7
1148-STF	18	35.3 ± 1.7	52.0 ± 2.5	33.9 ± 3.8	49.8 ± 5.6
1148-STF	23	11.5 ± 0.5	13.9 ± 0.6	13.2 ± 0.3	12.7 ± 0.6

Similar trends are observed with the STF intercalated assemblages when the inter-layer friction is enhanced. With the 1148-STF assemblages, there is no statistically significant change in the peak force or energy dissipation due the enhancement of inter-layer friction. This can again be rationalized through the tight nature of the correctional weave, which does not permit appreciable lateral displacement of yarns against the interlayer upon needle penetration. For the 1025-STF assemblages, enhancing the inter-layer friction increases the peak puncture force and energy dissipation over the neat assemblages with the thinner 18 gauge needle but results in a decrease in performance with the wider 14 gauge threat. These findings are qualitatively consistent with those of the untreated 1025 assemblages and they speak to the mechanistic role of both STF intercalation and inter-layer friction enhancement during needle penetration of ballistic fabrics. Upon needle penetration, the STF between fibrils can enhance energy dissipation through viscous dissipation and decreased intra-layer yarn mobility. Simultaneously, the lateral motion of yarns displacing away from the needle is resisted by friction from the

interlayer which also contributes to energy dissipation. For the thinner 18 gauge needle, the combined effects of STF intercalation and enhanced inter-layer friction work synergistically to improve the performance of the assemblage. However, the ability of the STF to contribute to energy dissipation requires that the yarns remain intact. Once yarn and fiber breakage occurs, the STF loses its ability to contribute to energy dissipation. This is reflected in the results of the 1025-STF assemblages penetrated by the wider 14 gauge threat. Yarn and fiber breakage is induced by the enhanced inter-layer friction and the STF loses its ability to dissipate energy.

As discussed in the introduction, friction during an impact event can take many forms, and as noted, much attention has been paid to intra-yarn and inter-yarn friction, while comparatively little study has been devoted to inter-layer friction. Here we show incorporation of enhanced inter-layer friction into a ballistic textile assemblage can improve the resistance to narrow widowing threats. However, in situations where the penetrator is of lower gauge, enhanced inter-layer friction can hinder other frictional mechanisms from contributing to the overall energy dissipation of the assemblage. The results of this study should therefore motivate consideration of the role of inter-layer friction in the design of ballistic textile assemblages.

Conclusions

The effects of STF intercalation and inter-layer friction enhancement on the needle puncture resistance of protective textile lay-ups are quantified. STF intercalation was shown to improve resistance to quasi-static hypodermic needle puncture with the largest percentage improvement observed for ballistic textiles. In contrast, the effect of increasing inter-layer friction was found to exhibit a dependence on the architecture of the fabric and the needle gauge.

It was postulated that an optimum level of inter-layer friction exists that resists windowing of the penetrating needle without inducing yarn breakage. These results are qualitatively similar to those observed for complementary studies of inter-yarn friction [9, 30]. Assemblages of textiles intercalated with STF and enhanced inter-layer friction demonstrated a similar behavior, and as such, inter-layer friction was identified as a critical factor that affects energy dissipation and can possibly affect other frictional energy dissipation mechanisms within the assemblage. Ultimately, this work provides a better understanding of how inter-layer friction can be engineered into a ballistic textile assemblage to improve its puncture resistance. Future work will extend this investigation to study the role of inter-layer friction against stab and ballistic threats.

Acknowledgement

The authors would like to thank Dr. Aadil Elmoumni and TA Instruments for use of the tribology cell adaptor. This work was supported by a NASA EPSCoR Grant (NNX11AQ28A) and a Delaware Space Grant Graduate Fellowship (NNX10AN63H).

References

1. Tabiei, A. and G. Nilakantan, *Ballistic impact of dry woven fabric composites: A review.* Applied Mechanics Reviews, 2008. **61**(1): p. :010801-010813.

2. Roylance, D., A. Wilde, and G. Tocci, *Ballistic Impact of Textile Structures.* Textile Research Journal, 1973. **43**(1): p. 34-41.

3. Kirkwood, K.M., et al., *Yarn pull-out as a mechanism for dissipating ballistic impact energy in Kevlar((R)) KM-2 fabric - Part I: Quasi-static characterization of yarn pull-out.* Textile Research Journal, 2004. **74**(10): p. 920-928.

4. Kirkwood, J.E., et al., *Yarn pull-out as a mechanism for dissipating ballistic impact energy in Kevlar((R)) KM-2 fabric - Part II: Predicting ballistic performance.* Textile Research Journal, 2004. **74**(11): p. 939-948.

5. Cheeseman, B.A. and T.A. Bogetti, *Ballistic impact into fabric and compliant composite laminates.* Composite Structures, 2003. **61**(1-2): p. 161-173.

6. Shim, V.P.W., V.B.C. Tan, and T.E. Tay, *Modeling Deformation and Damage Characteristics of Woven Fabric under Small Projectile Impact.* International Journal of Impact Engineering, 1995. **16**(4): p. 585-605.

7. Prosser, R.A., S.H. Cohen, and R.A. Segars, *Heat as a factor in the penetration of cloth ballistic panels by 0.22 caliber projectiles.* Textile Research Journal, 2000. **70**(8): p. 709-722.

8. Lee, B.L., et al., *Penetration failure mechanisms of armor-grade fiber composites under impact.* Journal of Composite Materials, 2001. **35**(18): p. 1605-1633.

9. Hearle, J.W.S., et al., *Ballistic Impact Resistance of Multi-Layer Textile Fabrics*, 1981, University of Manchester Institute of Science and Technology.

10. Mewis, J. and N.J. Wagner, *Colloidal Suspension Rheology* 2012, New York: Cambridge University Press.

11. Bender, J. and N.J. Wagner, *Reversible shear thickening in monodisperse and bidisperse colloidal dispersions.* Journal of Rheology, 1996. **40**(5): p. 899-916.

12. Lee, Y.S. and N.J. Wagner, *Rheological properties and small-angle neutron scattering of a shear thickening, nanoparticle dispersion at high shear rates.* Industrial & Engineering Chemistry Research, 2006. **45**(21): p. 7015-7024.

13. Maranzano, B.J. and N.J. Wagner, *Flow-small angle neutron scattering measurements of colloidal dispersion microstructure evolution through the shear thickening transition.* Journal of Chemical Physics, 2002. **117**(22): p. 10291-10302.

14. Decker, M.J., et al., *Stab resistance of shear thickening fluid (STF)-treated fabrics.* Composites Science and Technology, 2007. **67**(3-4): p. 565-578.

15. Kalman, D.P., et al., *Effect of Particle Hardness on the Penetration Behavior of Fabrics Intercalated with Dry Particles and Concentrated Particle-Fluid Suspensions.* Acs Applied Materials & Interfaces, 2009. **1**(11): p. 2602-2612.

16. Wagner, N.J. and E.D. Wetzel, *Advanced Body Armor Utilizing Shear Thickening Fluids*, US Patent 7,226,878. University of Delaware, 2007.

17. Wagner, N.J. and E.D. Wetzel, *Advanced Body Armor*, US Patent 7,825,045. University of Delaware, 2010.

18. Lee, Y.S., E.D. Wetzel, and N.J. Wagner, *The ballistic impact characteristics of Kevlar (R) woven fabrics impregnated with a colloidal shear thickening fluid.* Journal of Materials Science, 2003. **38**(13): p. 2825-2833.

19. Liang-Liang Sun, D.-S.X., Cai-Yun Xu, *Application of Shear Thickening Fluid in Ultra High Molecular Weight Polyethylene Fabric.* Journal of Applied Polymer Science, 2013. **129**(4): p. 1922-1928.

20. Kang, T.J., C.Y. Kim, and K.H. Hong, *Rheological behavior of concentrated silica suspension and its application to soft armor.* Journal of Applied Polymer Science, 2012. **124**(2): p. 1534-1541.

21. Park, J.L., et al., *Ballistic performance of p-aramid fabrics impregnated with shear thickening fluid; Part I - Effect of laminating sequence.* Textile Research Journal, 2012. **82**(6): p. 527-541.

22. Park, J.L., et al., *Ballistic performance of p-aramid fabrics impregnated with shear thickening fluid; Part II - Effect of fabric count and shot location.* Textile Research Journal, 2012. **82**(6): p. 542-557.

23. Mead, W.J., *The geologic role of dilatancy.* Journal of Geology, 1925. **33**(7): p. 685-698.

24. Gates, L.E., Jr. , *Flexible Protective Armour Material and Method of Making Same*, US Patent 3,649,426. Hughes Aircraft Company, 1972.

25. McAllister, Q.P., J.W. Gillespie, and M.R. VanLandingham, *The influence of surface microstructure on the scratch characteristics of Kevlar fibers.* Journal of Materials Science, 2013. **48**(3): p. 1292-1302.

26. Wetzel, E.D., et al. *The Effect of Rheological Parameters on the Ballistic Properties of Shear Thickening Fluid (STF)-Kevlar Composites*. in *8th International Conference on Numerical Methods in Industrial Forming Processes*. 2004. Columbus, OH.

27. Rao, M.P., et al., *Modeling the effects of yarn material properties and friction on the ballistic impact of a plain-weave fabric.* Composite Structures, 2009. **89**(4): p. 556-566.

28. Duan, Y., et al., *Modeling friction effects on the ballistic impact behavior of a single-ply high-strength fabric.* International Journal of Impact Engineering, 2005. **31**(8): p. 996-1012.

29. Duan, Y., et al., *A numerical investigation of the influence of friction on energy absorption by a high-strength fabric subjected to ballistic impact.* International Journal of Impact Engineering, 2006. **32**(8): p. 1299-1312.

30. Zeng, X.S., V.B.C. Tan, and V.P.W. Shim, *Modelling inter-yarn friction in woven fabric armour.* International Journal for Numerical Methods in Engineering, 2006. **66**(8): p. 1309-1330.

31. Nilakantan, G. and J.W. Gillespie, *Ballistic impact modeling of woven fabrics considering yarn strength, friction, projectile impact location, and fabric boundary condition effects.* Composite Structures, 2012. **94**(12): p. 3624-3634.

32. Briscoe, B.J. and F. Motamedi, *The Ballistic Impact Characteristics of Aramid Fabrics - the Influence of Interface Friction.* Wear, 1992. **158**(1-2): p. 229-247.

33. Mayo, J.B., et al., *Stab and puncture characterization of thermoplastic-impregnated aramid fabrics.* International Journal of Impact Engineering, 2009. **36**(9): p. 1095-1105.

34. Gadow, R. and K. von Niessen, *Lightweight ballistic with additional stab protection made of thermally sprayed ceramic and cermet coatings on aramide fabrics.* International Journal of Applied Ceramic Technology, 2006. **3**(4): p. 284-292.

35. Chitrangad, M.a.R.-P., J., *Fluorinated Finishes for Aramids*, 1993, E.I. du Pont de Nemours and Company.

36. Hassim, N., et al., *Puncture resistance of natural rubber latex unidirectional coated fabrics.* Journal of Industrial Textiles, 2012. **42**(2): p. 118-131.

37. Termonia, Y., *Puncture resistance of fibrous structures.* International Journal of Impact Engineering, 2006. **32**(9): p. 1512-1520.

38. Houghton, J.M., et al. *Hypodermic Needle Puncture of Shear Thickening Fluid (STF)-Treated Fabrics*. in *SAMPE*. 2007. Baltimore, MD.

39. Dombrowski, R.D. and N.J. Wagner, *Measurement of Needle Punture Resistance Using an Electronic Puncture Detection System*, in *SAMPE*: Baltimore, MD. 2012.

40. Kavehpour, H.P. and G.H. McKinley, *Tribo-rheometry: from gap-dependent rheology to tribology.* Tribology Letters, 2004. **17**(2): p. 327-335.